

Cluster observations during pseudo-breakups and substorms

A. Runov, I. O. Voronkov, Y. Asano, R. Nakamura, W. Baumjohann, M. Volwerk, T. Takada, Z. Voros, T. L. Zhang, A. Vaivads, S. Haaland, H. Rème, and A. Balogh

Abstract: We discuss Cluster observations of the magnetotail plasma sheet during a set of successive auroral activations between 0300 and 0600 UT on September 15, 2001. Cluster was located near the midnight meridian at about $19 R_E$ downtail, with foot points on the CANOPUS network, staying in the plasma sheet. Analyzing Cluster magnetometer and ion spectrometer data, we found that the activity in the plasma sheet starts after a 2.5 hours long interval of B_z decrease; the pseudo-breakups and small substorms, detected by CANOPUS, are associated with enhancements of tailward ion flow. The substorm, following the pseudo-breakups, corresponds to a high-speed ion flow reversal from tailward to Earthward, with a quadrupolar magnetic field structure and intensive ion heating. Thus, the substorm is associated with magnetic reconnection in the near-Earth ($X > -19 R_E$) plasma sheet. The current sheet half-thickness, estimated using four-point magnetic field measurements, gradually decreased prior to the flow reversal, achieving a minimum (less than 1000 km) at expansion phase onset. Finally, the excitation of quasi-harmonic waves with periods of 150 - 200 s, propagating duskward with velocities of 50 - 100 km/s, was detected by the Cluster magnetometers during and after the flow enhancements. Since the IMF was mostly northward, the plasma sheet disturbances during this interval were most likely internally triggered.

Key words: Substorms, Pseudo-breakups, Current sheet, Reconnection.

1. Introduction

In situ observations in the mid tail plasma sheet are important for understanding physical mechanisms of energy conversion during magnetospheric substorms and substorm-like activations. Key issues are the evolution of the magnetotail current sheet structure and the spatial localization of instabilities, responsible for burst-like energy release. Numerous previous studies with single spacecraft or occasional spacecraft constellations gave the basic information to construct physical models of a substorm. For example, ISEE-1/2 observations show temporal changes of the magnetotail current sheet thickness and structure [1] and formation of a thin current sheet prior to expansion phase [2]; observations by the Geotail spacecraft allowed to place the most probable location of a reconnection region associated with substorm onset between $X = -20 - -30 R_E$ and $0 < Y < 8 R_E$ [3, 4, 5].

The four Cluster spacecraft have polar orbits with apogee at $\sim -19 R_E$. Forming a quasi-regular tetrahedron in the magnetotail, Cluster enable to identify moving spatial structures like boundary layers, current sheets, wave and flow burst fronts. Four-point timing analysis [6] allows to determine the direction of the spatial structures motion. Therefore, Cluster ob-

servations may provide information about meso-scale (with scales in between several hundreds and several thousands km) transient structures, their internal structure and motion during substorm-like events.

This paper presents a detailed analysis of four-point Cluster observations during a set of successive pseudo-breakups and substorms between 0300 and 0600 UT on September 15, 2001. We will focus on the detection of spatial structures and characterization of their motion. A description and analysis of ground-based observations, IMAGE and GOES spacecraft measurements are contained in the accompanied paper by Voronkov et al., this issue.

2. Overview

The overview plot for interval 0000 - 0600 UT on September 15, 2001 is presented in Fig. 1. The IMF B_z (Wind and Geotail data, Fig. 1, a, X and Y_{GSM} positions are specified on the plot) was southward during 0000 - 0045 UT, turned northward at 0045 - 0050 and stays mainly northward except for short excursions at about 0400 and 0530 UT. The substorm with the AL peak of -700 nT (Fig. 1, b) was observed between 0000 - 0050 UT. After the northward turning of the IMF, the AL index decreases to zero. The activity starts again apparently without external triggering at ~ 0340 UT, with a drop of H_e and a local increase of H_p detected by GOES-8 at geostationary orbit (the vertical dashed line in Fig. 1).

During 0000 - 0600 UT the Cluster quartet traveled between $[-18.9, 3.5, 1.1]$ and $[-18.5, 3.3, -3.4] R_E$ (barycenter, GSM coordinates), forming a nearly regular tetrahedron with the largest inter-spacecraft distance of 1700 km (Fig. 1, uppermost panel). The X_- and Z_- (GSM coordinates are used overall the paper) components of the magnetic field from the Cluster Fluxgate Magnetometer (FGM, [7]) at the most northern (C4, thick line)

Received 17 May 2006.

A. Runov, R. Nakamura, W. Baumjohann, M. Volwerk, T. Takada, Z. Voros, and T. L. Zhang. Space Research Institute Austrian Academy of Sciences, Schmiedlstrasse 6, A-8042 Graz, Austria
I. O. Voronkov. University of Calgary, Calgary, Canada
Y. Asano. Tokyo Institute of Technology, Tokyo, Japan
A. Vaivads. Swedish Institute of Space Physics, Uppsala, Sweden
S. Haaland. MPE, Garching, Germany
H. Rème. CESR/CNRS, Toulouse, France
A. Balogh. Imperial College, London, UK

and most southern (C3, thin line) spacecraft are plotted in Fig. 1, (panels e and f). The ion time-energy spectrogram and proton bulk velocity from Cluster Ion Spectrometry experiment (CIS, [8]) are presented in Fig. 1 g and h. Fig. 1 d shows the magnetic field strength in the lobe, estimated from the FGM and CIS data assuming pressure balance. During the substorm between 0000 - 0050 UT Cluster observed a set of Earthward high speed bulk flow bursts followed by strong dipolarization in the mid-tail plasma sheet ($B_z \sim 15$ nT). Between 0100 - 0340 UT Cluster observed a gradual decrease of B_z down to zero and increase of the magnetic field gradient (difference between B_x at C3 and C4). The ion flow is near zero level and ion temperature gradually decreases.

After ~ 0340 UT the activity in the plasma sheet arises again: Cluster detects a sequence of three successive tailward high-speed ion flow bursts followed by high-speed flow reversal. During approximately 0300 - 0600 UT Cluster foot points were conjuncted to the CANOPUS network. The observations on CANOPUS (see Voronkov et al., this issue) show the set of successive small local substorms and pseudo-breakups associated with the tailward ion flow bursts between 0340 - 0445 UT and a moderate full developed substorm during the ion flow reversal at 0455 - 0535 UT.

Further we discuss Cluster observations during small substorms and pseudo-breakups (0340 - 0445 UT) and during the substorm interval (0455 - 0535 UT) separately.

3. Cluster Observations During Small Substorms and Pseudo-Breakups

Fig. 2 presents the Cluster observations in the magnetotail plasma sheet during 0315 - 0445 UT on September 15, 2001. Before the activity starts at 0340 UT, the magnetotail current sheet at the Cluster orbit was stable and quasi-1D, with the gradient directed dominantly along Z . The half-thickness of the current sheet, estimated using the Harris function (HL) varies between 1 - 2 R_E , showing a breathing of the sheet. Ion flows in the plasma sheet are at the near-zero level and the lobe field is stable at a level of 36 nT, indicating rather quiet plasma sheet prior to the activation.

The situation changes dramatically at 0341 UT (vertical dashed line), when the 370 s. long tailward flow burst with velocity of -400 km/s at 0345 UT and large-amplitude variations of the magnetic field were detected by Cluster. The tailward flow burst was followed by the negative variation of B_z with minimum of -10 nT, bipolar variations of B_y (mainly negative during the tailward flow). B_x first slightly increases then abruptly drops to zero. The quasi-1D current sheet structure changes abruptly to a complex 3D one with all three components of the electric current density vary between -5 - 5 nA/m². The current sheet half-thickness estimation using the Harris function can not be meaningfully made during this interval. The energy of ions increases, some exceeding the CIS energy range (40 keV). The estimated lobe field first increases, has a local minimum, increases again up to 38 nT and then decreases down to 32 nT. The Y -component of the convection electric field, estimated as $-\mathbf{V} \times \mathbf{B}$ increases up to 3.5 mV/m (Fig 1, i), indicating that the tailward flow carries a significant amount of the magnetic flux.

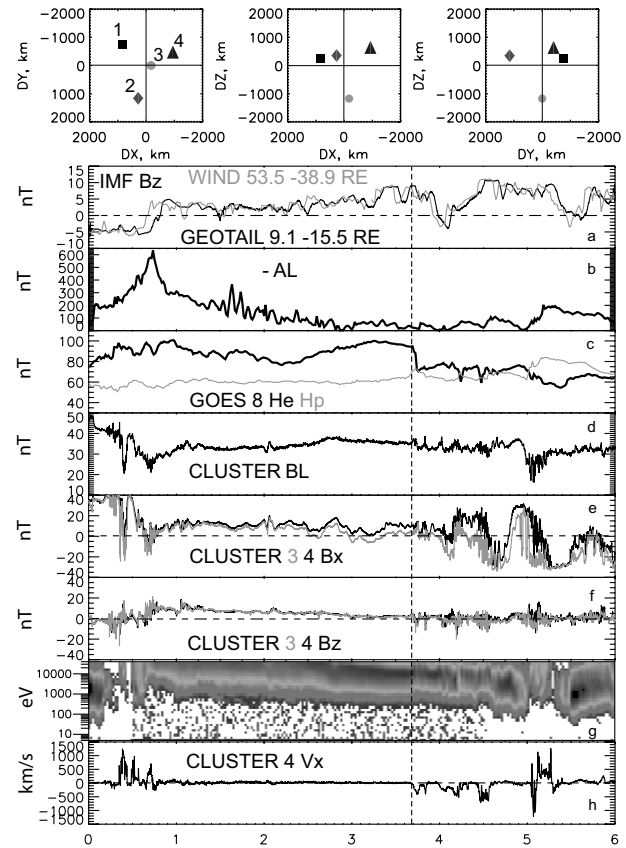


Fig. 1. September 15, 2001: The Cluster tetrahedron configuration in respect for the tetrahedron barycenter and event overview plot: IMF B_z at Wind and Geotail (a), abs. values of AL -index from Kyoto monitor (b), p - and e - components of the magnetic field at geostationary orbit (c), the magnetic field strength in the lobe estimated from the Cluster CIS and FGM data (d), B_x and B_z (GSM) at Cluster 3 (thin) and 4 (thick) (e and f, respectively), ion energy-time spectrogram from Cluster 1 (g), X -component of the ion bulk velocity at Cluster 4 (h).

At ~ 0350 UT Cluster detected the next tailward ion flow burst with duration of 150 s and velocity of -400 km/s. B_x at Cluster 1, 2 and 4 increases up to 17 nT, while B_x at Cluster 3 stays around zero. B_y at Cluster 1,2 and 4 shows a negative excursion down to -16 nT, while B_y at Cluster 3 varies in the range of ± 3 nT. B_z at all four spacecraft shows bipolar variation, associated with minimum of B_y . The corresponding current density increases up to 10 nA/m², with positive peaks of j_y and j_x and bipolar variation of j_z . The lobe magnetic field strength locally increases up to 39 nT. These signatures allow interpreting this structure as the tailward propagating flux rope [9]. The Harris estimate of the half-thickness of this structure locally decreases down to 3000 km.

During 0359 - 0417 UT Cluster observed the tailward ion flow with velocity varying between -600 and -200 km/s with two distinct velocity enhancements, corresponding to two different auroral activations (see Voronkov et al., this issue). The first flow enhancement was detected at about 100 s earlier than the magnetic field variations. At the very beginning of the flow interval B_x at Cluster 3 was around zero and the other three

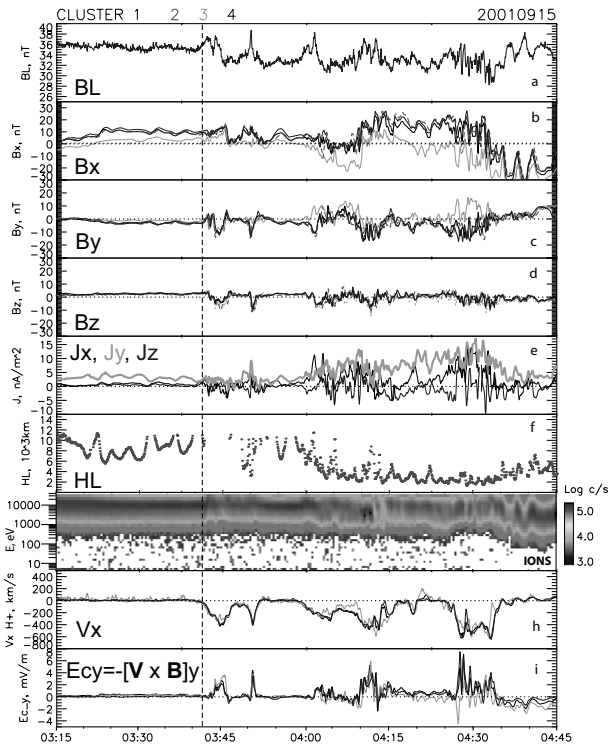


Fig. 2. Estimated lobe magnetic field (a), X -, Y - and Z -components of the magnetic field (GSM) (b,c,d) from Cluster 1 (solid black), 2 (dashed), 3 (gray) and 4 (thin black), X -, Y - and Z -components of the calculated current density (e), estimated half-thickness of the current sheet in 10^3 km (f), time-energy spectrogram, Cluster 1 (g), X -component of the ion bulk velocity (h), and calculated convective electric field (i) versus UT.

spacecraft detect $B_x \sim 5$ nT. At the same time, B_y at Cluster 3 locally increases up to ~ 10 nT, and B_y at Cluster 1, 2 and 4 locally decreases down to ~ -10 nT; B_z at all four spacecraft exhibits a bipolar variation from positive to negative. The lobe field strength has a local peak of 38 nT. The magnetic field data are consistent with a dawnward ($-Y$) motion of the X -directed current. About 1.5 min later on, at 0403 UT, Cluster 2 shows a negative excursion of B_x down to -10 nT and positive excursion of B_y up to 10 nT, Cluster 4, a positive variation of B_x up to 10 nT and a negative one of B_y down to -10 nT, while B_x and B_y at Cluster 1 vary between -2 and 5 nT, B_x and B_y at Cluster 3 stay at about -10 nT and ~ 10 nT, respectively. B_z at all four probes reverses from negative to positive. These observations can be interpreted as signatures of tailward propagation of the Z -directed current filament. The estimated thickness of the current sheet decreases down to ~ 2000 km. At 0405 UT, B_x and B_y at all four spacecraft are close to zero, while B_z trace from Cluster 2 differs from the others, indicating a presence of the current, directed tailward ($-X$). At ~ 0410 UT Cluster crossed a relatively thin current sheet with current density increasing up to 14 nA/m². Assuming that this current sheet is a planar boundary, four-point timing gives an estimate of the boundary normal velocity $[0.0, 0.53, -0.85] \cdot 83$ km/s: The current sheet moves south- and dusk-ward. Estimated half-thickness of the sheet is about

2500 km. The tailward flow velocity increases to 500 km/s, and Cluster/CIS detects a short increase of plasma density with decrease of ion energy. The convection electric field increases up to 6 mV/m.

During 0425 - 0435 UT, Cluster observed tailward ion flow with velocity of -600 km/s. The magnetic field is strongly fluctuating, with amplitude of fluctuations of 15 - 20 nT. B_x is mainly negative at Cluster 3 and positive at the three others. $B_y > 0$ at Cluster 3 and $B_y < 0$ at the three others. B_z is mainly negative at the all four. The electric current directed mainly along Y with significant positive X . j_z experiences bipolar variation, indicating the current sheet corrugation in YZ plane. The current density reaches 18 nA/m², and the estimated half-thickness of the current sheet decreases down to 1500 - 2000 km. Energy of ions increases to ~ 8 keV during this interval.

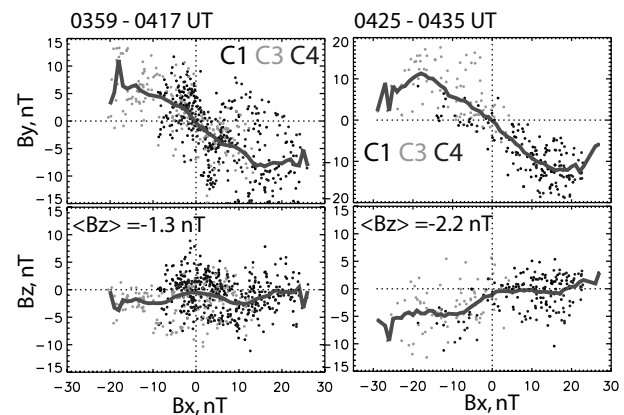


Fig. 3. Y - (upper row) and Z - (bottom row) components of the magnetic field at Cluster 1, 3, and 4 versus B_x for 0359 - 0417 and 0425 - 0435 UT. Samples with $V_x < -100$ km/s are used only. The thick lines show the average values in each 2 nT bin.

During the tailward fast flows intervals 0359 - 0417 UT and 0425 - 0435 UT the magnetic field at the most southern spacecraft (Cluster 3) was smaller and at the most northern one (Cluster 4) was larger than at the others, which is consistent with their GSM location (Fig., 1, uppermost panel). Thus, the GSM system is an appropriate proxy for the current sheet normal coordinate system. Fig. 3 shows Y and Z components of the magnetic field from Cluster 1, 3 and 4 corresponding to $V_x < -100$ km/s versus B_x . For both intervals B_z is positive in the southern half and negative in the northern half of the sheet, while B_z is predominantly negative, which is consistent with the quadrupolar out-of-plane field pattern at tailward side of reconnection site [3]. The same analysis applied to the first two flow bursts (0341 and 0350 UT) does not show any regular behavior of B_y and B_z in respect to B_x .

Fig. 4 presents low-pass filtered B_x and B_z time series from all four Cluster spacecraft and V_x time series from Cluster 1, 3 and 4. Note, that time (in seconds after 0340:00 UT) increases from right to left in this plot. It is visible from the presented data that the ion bulk flow enhances instantaneously with B_z reversals from some positive value to a negative one. Considering the B_z reversals as a signatures of a spatial boundary, separating accelerated plasma flow carrying the southward

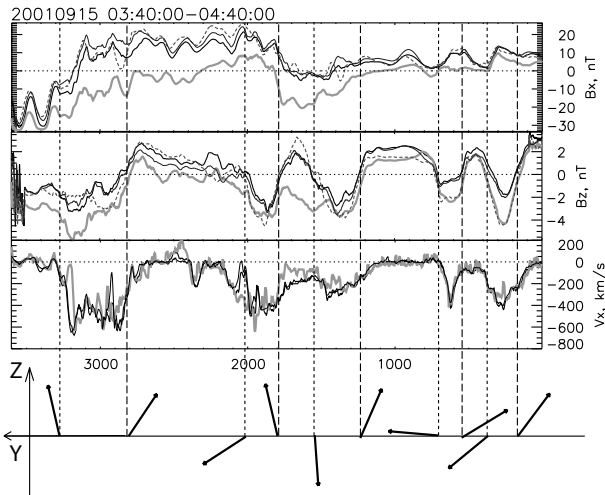


Fig. 4. Low-pass filtered B_x and B_z reverse time series from all Cluster spacecraft, V_x from Cluster 1, 3 and 4, and YZ_{GSM} projections of normal vector resulting from B_z timing analysis.

magnetic field and a quiet plasma with predominantly northward B_z , we performed four-point timing analysis to determine directions of these boundaries motion. The analysis shows that the boundaries moves mainly in YZ plane (Fig. 4, bottom panel), indicating up-down and dawn-dusk motion. The inward boundary crossings with $B_z > 0 \rightarrow B_z < 0$ variations are associated with upward ($+Z$) and mainly downward motion of the boundaries while the outward crossings - with duskward and downward, except for the last (most left-hand-side) reversal. Thus Cluster was situated above and downward of the flow channel, expanding during the flow enhancements. Cluster crossed the flow channel during the tailward flow between 0425-0435 UT.

Quasi-periodic oscillations with period of 2-3 min were observed by Cluster/FGM during $\sim 0400 - 0445$ UT. They become more pronounced during and after the boundary crossing at ~ 0410 UT. Timing of the magnetic field traces show that the oscillations are slowly propagating duskward with velocity of several tens km/s. The nice looking train of the oscillations with $T \sim 180$ s during 0435 - 0445 UT allows to perform more precise timing analysis which gives the duskward propagating velocity of 60-70 km/s.

4. Cluster Observations During the Substorm

Fig. 5 shows an hour of Cluster data during the substorm interval 0445 - 0545 UT. The vertical dashed line at ~ 0454 UT indicates the substorm onset, observed at PBQ (see Voronkov et al., this issue).

Before the substorm onset, during 0445 - 0454 UT, all four Cluster spacecraft cross the quiet current sheet (from $B_x = -20$ nT to $B_x \sim 25$ nT). B_y anti-correlates with B_x , changing from positive to negative values during the sheet crossing. B_z also changes from a small negative value in southern half to a positive one in the northern half of the sheet. Timing analysis of the magnetic field time series shows the current sheet normal direction $\mathbf{N} = [0.20, -0.05, -0.98]$ (the $N_z < 0$ indicates southward motion of the current sheet during the crossing). The nor-

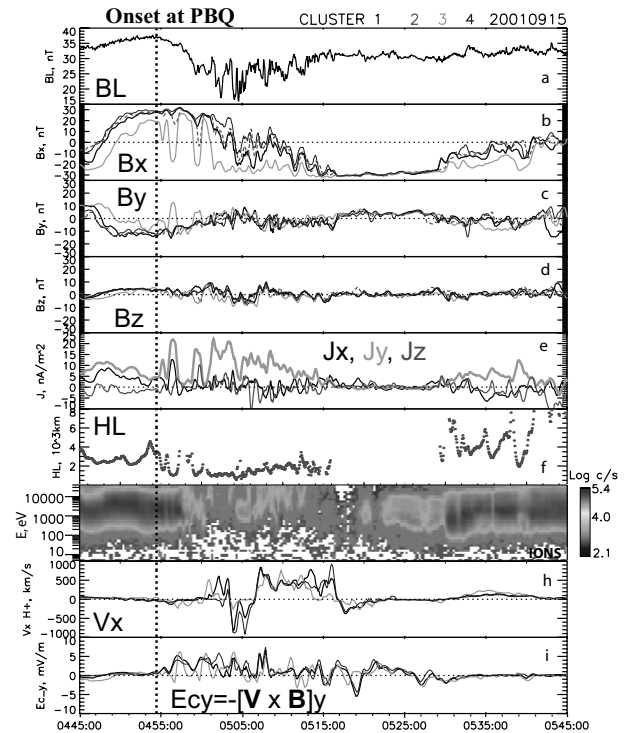


Fig. 5. The same as in Fig. 2 for the substorm interval 0445 - 0545 UT.

mal velocity of the sheet motion, estimated by timing, is very small, about 10 - 15 km/s. Minimum Variance Analysis (MVA, [10]), being applied for the magnetic field time series of all four spacecraft, gives essentially the same results with the normal directed basically along Z and the main field (the maximum variance eigenvector) along $\mathbf{L} = [0.9, -0.5, 0.1]$, indicating the significant shear component of the magnetic field at $\sim 3.4 R_E$ from midnight. The current density reaches 13 nA/m^2 with current directed in Y and X and a local minimum of the current density at $B_x = 0$ at the Cluster barycenter. The estimated current sheet half-thickness is about 3000 km. The lobe field slightly increases from 34 to 38 nT. The count rate locally increases at ion energies between 2 and 5 keV during 0446 - 0453 UT.

Immediately after substorm onset, during 0454 - 0502 UT, Cluster observed a train of magnetic field variations with a quasi-period of 180 s and amplitude up to 25 nT. The largest variations with change of the magnetic field polarity were observed by the most southern spacecraft (Cluster 3). Assuming that these variations are due to the current sheet kinking and that the current sheet is a plane boundary during the kinking, application of timing analysis shows that the kinks propagate duskward with the normal velocity about 60 km/s. The large shear of the magnetic field persists during the kinking: Cluster 3 detects $B_y > 0$ during excursions to the southern half of the sheet while the others, staying in the northern half, show $B_y < 0$. B_z varies between -12 and 10 nT, displaying bipolar variations, coinciding with the B_x variations. Current density increases up to 22 nA/m^2 , and the corresponding current sheet half-thickness drops down to about 1000 km. The estimated lobe field strength decreases from 38 to 18 nT. The electric

field $E_{cy} = -(V_z B_x - V_x B_z)$ increases up to 5 mV/m, indicating a considerable vertical flux transfer.

During 0501 - 0504 UT Cluster observed a thin current sheet: B_x at Cluster 3 varies around -23 nT, while Cluster 4, located in 1739 km northern, detected $15 \leq B_x \leq 20$ nT. Cluster 1 and 2, located almost at the same Z , show similar magnetic field behavior crossing the neutral sheet. The current density, estimated using the Linear Gradient Estimator technique [11] varies in the range 15 - 22 nA/m². Using the differences between B_x at Cluster 1 and 2 as a proxy of the inner sheet current density and Cluster 3 and 4 as one of the entire sheet, we have found 85 nA/m² and ~ 18 nA/m², respectively. The CIS/HIA count rate at Cluster 1 decreases dramatically, showing an absence of low-energy ions in the thin sheet. Calculated moments, however questionable because of low density, show Earthward flow enhancements at Cluster 1 and 3.

Between 0504 and ~ 0517 UT, the ion bulk flow reversal from tailward ($V_x \sim -900$ km/s) to Earthward ($V_x \sim 800$ km/s) was observed by Cluster 1, 3 and 4. The ion time-energy spectrogram shows a presence of mixed low- (1 - 3 keV) and high-energy (≥ 10 keV) population. B_x at Cluster 1, 2 and 4 first varied between -20 and 10 nT, then decreased down to -30 nT at the end of the flow reversal interval. B_x at Cluster 3 varied in the range -20 - -30 nT. B_y and B_z were fluctuating during this interval, B_z was mainly negative during the tailward flow and mainly positive at the beginning of the Earthward flow.

Fig. 6 shows the scatter plots of V_x at Cluster 1 and 4 versus X -component of the magnetic field curvature vector $\mathbf{C} = (\mathbf{b} \cdot \nabla)\mathbf{b}$ and X -component of the Lorentz force $\mathbf{F}_L = \mathbf{j} \times \mathbf{B}$. Points are clearly concentrated in bottom left ($V_x < 0$, $C_x < 0$, $F_{Lx} < 0$) and upper right quadrants ($V_x > 0$, $C_x > 0$ and $F_{Lx} > F_0$, showing signatures typical for magnetic X -line configuration (e.g., [12]).

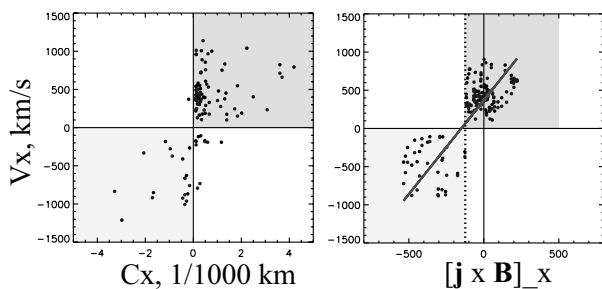


Fig. 6. Left-hand panel: X -component of the ion bulk velocity versus X -component of the magnetic field curvature vector; right-hand panel: X -component of the ion bulk velocity versus X -component of the Lorentz force during the flow-reversal interval 0504 - 0517 UT.

Fig. 7 shows B_y and B_z at Cluster 1, 3, and 4 versus B_x for the tailward flow ($V_x < -100$ km/s) and for the Earthward flow ($V_x > 100$ km/s) intervals. During the tailward flow $B_y > 0$ at $B_x < 0$ and $B_y < 0$ at $B_x > 0$, while $B_z < 0$. This behavior is consistent with the Hall quadrupolar field pattern tailward of X -line. During the Earthward flow, contrary, $B_y > 0$ at $B_x < 0$ in agreement with the Hall pattern Earthward of the X -line [3].

It is interesting to note that after a stay in the southern lobe and/or PSBL during 0517 - 0529 UT Cluster entered into re-

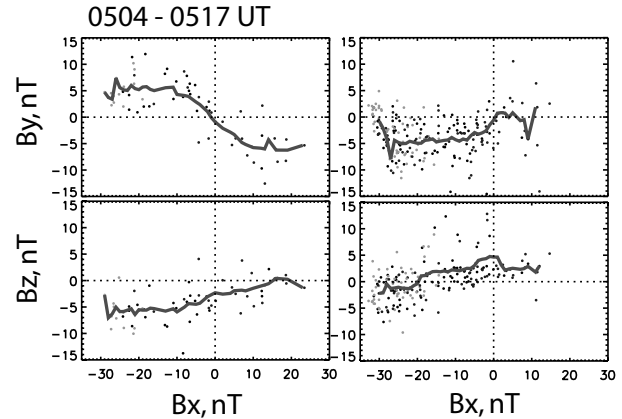


Fig. 7. Y - (upper row) and Z - (bottom row) components of the magnetic field at Cluster 1, 3 and 4, samples with corresponding $V_x < -100$ km/s (left column) $V_x > 100$ km/s (right column) versus corresponding B_x during the flow reversal interval 0504 - 0517 UT. The thick lines show the average values in each 2 nT bin.

latively cold and dense plasma sheet. The ion energy spectrum after 0529 UT is similar to one observed during 0445 - 0459 UT before the substorm onset. Therefore during the substorm, Cluster crossed the spatially localized rarefied volume of the plasma sheet populated by hot accelerated rarefied plasma embedded into colder and denser plasma sheet. Fig. 8 shows B_x , low-pass filtered normalized spacecraft potential U from Cluster/EFW [13], which may be used as a proxy of the particle density [14] (applications of this technique to the magnetopause are discussed in [15]) and ion number density from Cluster/CIS during 0450 - 0540 UT. Although Active Spacecraft Potential Control (ASPOC, [16]) was on at Cluster 3 and 4 the normalized time series of the double probe U at four spacecraft may be used for approximate timing. Applying this, we found that the front of the rarefaction at 0459 UT was propagating tailward and downward with approximate normal velocity $[-0.9, -0.5, 0.1] * 50$ km/s.

5. Summary

Analyzing the Cluster observations at $X \simeq -19 R_E$ during the set of substorm-like activations, we found that five successive small local substorms (pseudo-breakups) were associated with tailward ion bulk flow bursts with duration varying from 3 to 15 min. The flow enhancement in the near-Earth magnetotail started without external triggering (IMF was northward, except for the short negative excursion at ~ 0400 , which may cause the forth activation) and was likely caused by internal instability in the near-Earth plasma sheet which may be resulted from the mid tail magnetic field stretching after the strong dipolarization during preceding substorm. The magnetic field transported by first two short flow bursts and by the first part of the third longer flow shows signatures of flux ropes, while the magnetic field during the second part of the third and during the forth tailward flow intervals displays the quadrupolar Hall field pattern, which may be interpreted as signatures of magnetic reconnection occurred in the near-Earth plasma sheet (Earthward

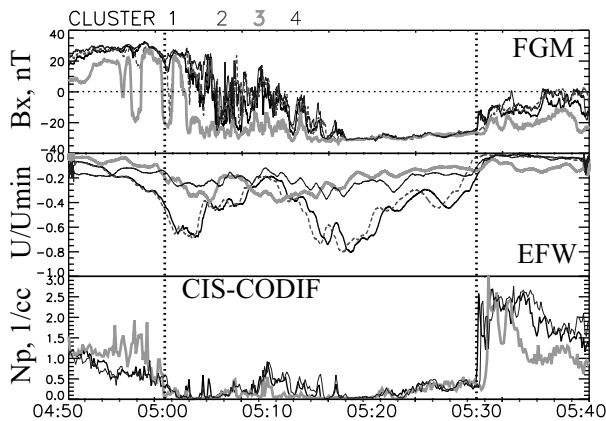


Fig. 8. X - component of the magnetic field (upper panel), low-pass filtered spacecraft potential (double probe), normalized by its minimum unfiltered value (mid panel) from all four Cluster spacecraft and proton number density from Cluster 1, 3 and 4 versus UT during the substorm interval.

of the Cluster position). Analysis shows that Cluster was situated upper and dawn-aside of the bulk flow channel, coming in the channel during flow enhancements.

The fully developed substorm following the set of pseudo-breakups was associated with high-speed flow reversal from tailward to Earthward, preceded by the magnetotail current sheet thinning. Analysis of the magnetic field and ion flow shows that plasma is accelerated by tailward and Earthward directed magnetic tensions. The signatures of the Hall current structure were found during tailward and Earthward parts of flow reversal. Therefore, tailward moving magnetic X -line was observed by Cluster during the substorm.

During the substorm, Cluster crossed a region in the mid tail plasma sheet populated by hot ions with much smaller number density, than in the surrounding relatively cold plasma sheet. This region of rarefied accelerated hot plasma moved tailward from the near-Earth plasma sheet.

Cluster four-point observations show that spatial structures (boundaries of flow channel, wave fronts, boundaries of the rarefaction region) move in cross-tail direction along with tail-Earthward motion. Therefore, simple 2-D cartoons, often used to describe the magnetotail dynamics during substorm-like events, are incomplete. Motions in third, cross-tail dimension seem to play an important role in the magnetotail plasma sheet dynamics.

Acknowledgements

We wish to thank H.-U. Eichelberger, G. Laky, M. Andre, C. Mouikis, L. Kistler, E. Georgescu and E. Penou for help with data and software, the ISSI Team 91 for fruitful discussion. The WIND and Geotail data are available on CDAWeb. We thank WDC for Geomagnetism, Kyoto providing AL indices. This work is supported by INTAS 03-51-3738.

References

1. Sergeev, V. A., Mitchell, D. G., Russell, C. T., and Williams, D. J., Structure of the tail plasma/current sheet at $\sim 11 R_E$

and its changes in the course of a substorm, *J. Geophys. Res.*, **98**, 17345–17365, 1993.

2. Sanny, J., McPherron, R. L., Russel, C. T., Baker, D. N., Pulkkinen, T. I., and Nishida, A.: Growth-phase thinning of the near-Earth current sheet during CDAW 6 substorm, *J. Geophys. Res.*, **99**, 5805–5816, 1994.
3. Nagai, T., Fujimoto, M., Saito, Y., Machida, S., Terasawa, T., Nakamura, R., Yamamoto, T., Mukai, T., Nishida, A., and Kokubun, S.: Structure and dynamics of magnetic reconnection for substorm onsets with Geotail observations, *J. Geophys. Res.*, **103**, 4419–4440, 1998.
4. Baumjohann, W., Hesse, M., Kokubun, S., Mukai, T., Nagai, T., and Petrukovich, A. A., Substorm dipolarization and recovery, *J. Geophys. Res.*, **104**, 24995 – 25000, 1999.
5. Nagai, T., Fujimoto, M., Nakamura, R., Baumjohann, W., Ieda, A., Shinohara, I., Machida, S., Saito, Y., and Mukai, Y. (2005), Solar wind control of the radial distance of the magnetic reconnection site in the magnetotail, *J. Geophys. Res.*, **110**, A09208, doi:10.1029/2005JA011207.
6. Harvey, C. C.: Spatial gradients and volumetric tensor, in: Analysis Methods for Multi-Spacecraft Data, edited by Paschmann, G. and Daly, P., pp. 307–322, ESA, Noordwijk, 1998.
7. Balogh, A., Carr, C. M., Acuña, M. H., et al., The Cluster magnetic field investigation: Overview of in-flight performance and initial results, *Ann. Geophys.*, **19**, 1207–1217, 2001.
8. Rème, H., Aostin, C., Bosqued, J. M., et al., First multispacecraft ion measurements in and near the Earth's magnetosphere with the identical Cluster ion spectrometry (CIS) experiment, *Ann. Geophys.*, **19**, 1303–1354, 2001.
9. Slavin, J. A., Lepping, R. P., Gjerloev, J., et al., Cluster electric current density measurements within a magnetic flux rope in the plasma sheet, *Geophys. Res. Lett.* **30**(7), 1362, doi:10.1029/2002GL016411, 2003.
10. Sonnerup, B. U. Ö. and Schneible, M., Minimum and maximum variance analysis, in: Analysis Methods for Multi-Spacecraft Data, edited by Paschmann, G. and Daly, P., pp. 185–220, ESA, Noordwijk, 1998.
11. Chanteur, G., Spatial interpolation for four spacecraft: Theory, in Analysis Methods for Multi-Spacecraft Data, edited by Paschmann, G. and Daly, P., pp. 349–369, ESA, Noordwijk, 1998.
12. Runov, A., Nakamura, R., Baumjohann, W., et al., Current sheet structure near magnetic X-line observed by Cluster, *Geophys. Res. Lett.*, **30**, 1579, doi:10.1029/2002GL016730, 2003.
13. Gustafsson, G., André, M., Carozzi, T., et al., First results of electric field and density observations by Cluster EFW based on initial months of operation, *Ann. Geophys.*, **19**, 1219–1240, 2001
14. Pedersen, A., Décréau, P., Escoubet, C.-P. et al., Four-point high time resolution information on electron densities by the electric field experiments (EFW) on Cluster, *Ann. Geophys.*, **19**, 1483–1489, 2001
15. Paschmann, G., Haaland, S., Sonnerup, B. U. Ö., Hasegawa, H., Georgescu, E., Klecker, B., Phan, T. D., Rème, H., and Vaivads, A., Characteristics of the near-tail dawn magnetopause and boundary layer, *Ann. Geophys.*, **23**, 1481–1497, 2005
16. Torkar, K., Riedler, W., Escoubet, C. P. et al., Active spacecraft potential control for Cluster - implementation and first results, *Ann. Geophys.*, **19**, 1289–1302, 2001.